Yang-Lee Distribution of Zeros for a van der Waals Gas

P. C. Hemmer and E. Hiis Hauge

Institutt for Teoretisk Fysikk, Norges Tekniske Høgskole, Trondheim, Norway

(Received 23 September 1963)

The distribution of zeros of the grand partition function for a gas obeying van der Waals' equation of state (together with Maxwell's rule) is studied. For infinite temperature the zero distribution is located on part of the negative real axis, but with decreasing temperatures the distribution branches off the real axis circumventing the origin on both sides. Below the critical temperature the distribution forms a closed curve around the origin with a diameter decreasing exponentially to zero as $T \to 0$. An additional tail of the distribution remains on the negative real axis at all temperatures, but with a density of zeros going linearly to zero with $T \to 0$.

INTRODUCTION

FOR a classical gas, Yang and Lee[1] have demonstrated that the equation of state of the condensed phases as well as the gas phase can be obtained from a knowledge of the distribution of zeros of the grand partition function as function of the fugacity z, in the limit of an infinite volume. However, the problem of determining this zero distribution is a formidable one. To the authors' knowledge the distribution is known in four cases only, viz. for (a) the one-dimensional lattice gas with nearest-neighbor interaction[2] (corresponds to the one-dimensional Ising ferromagnet), (b) the gas of hard rods,[3] (c) the gas with very weak repulsion of very long range,[3] and (d) the lattice gas with very weak attraction of very long range[4] (corresponds to a Bragg-Williams or Weiss field ferromagnet). Only the last model exhibits a phase transition.

It seems to us of interest, therefore, to study the properties of the zero distribution for a gas obeying van der Waals' equation

$$p = kT/(v-d) - a/v^2, \tag{1}$$

supplemented with the well-known Maxwell construction. The reason for choosing this equation of state is threefold: (i) It has a simple analytic form, (ii) it describes real gases qualitatively well, and (iii) it is
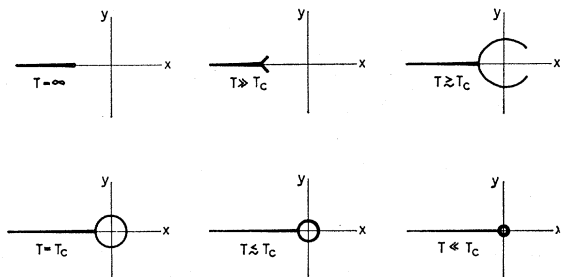

Fig. 1. The position of the zero distribution at different temperatures.

[1] C. N. Yang and T. D. Lee, Phys. Rev. **87**, 404 (1952).
[2] T. D. Lee and C. N. Yang, Phys. Rev. **87**, 410 (1952).
[3] E. H. Hauge and P. C. Hemmer, Physica (to be published).
[4] S. Katsura, J. Chem. Phys. **22**, 1277 (1954); Progr. Theoret. Phys. (Kyoto) **13**, 571 (1955).

rigorously the equation of state of a one-dimensional fluid model with pair interactions.[5] The interaction potential in this case consists of a hard core d and an attractive part to be considered in the limit when its strength $\to 0$ and its range $\to \infty$ so that the integral

$$\int_0^\infty dx \Phi^{\mathrm{attr}}(x) = a \tag{2}$$

has a finite value.

We rely heavily on the electrostatic analog devised by Lee and Yang.[2] The lines on which the zeros coalesce in the limit of an infinite volume are line charges in this picture. The logarithmic potential as determined by the equation of state is multiple valued, and the discontinuities in the electric field strengths across a charged line originate from joining two different Riemann sheets along the line.

The equations do not seem to allow a complete analytic solution, but rigorous results are obtained in limiting cases. In broad outline the movement of the zeros when the temperature decreases seems to be as indicated in Fig. 1.

2. THE ELECTROSTATIC POTENTIAL

We assume that in the limit of $V \to \infty$ the zeros of the grand partition function $Z_g(z,V,T)$ coalesce into lines C in the complex z plane, so that $Vg(s)ds$ is the number of zeros in the line element ds at $z = z(s)$. Then the well-known relation[1] between the equation of state and the zero distribution $g(s)$ is as follows:

$$p/kT = \chi(z) \tag{3}$$

$$\rho = z\chi'(z) \tag{4}$$

with

$$\chi(z) = \lim_{V \to \infty} \frac{\ln Z_g}{V} = \int_C g(s) \ln\left(1 - \frac{z}{s}\right) ds. \tag{5}$$

Here $\rho = 1/v$ is the number density.

The last relation displays the Lee-Yang interpretation of $\chi(z)$ as the complex logarithmic potential of charged

[5] M. Kac, G. E. Uhlenbeck, and P. C. Hemmer, J. Math. Phys. **4**, 216 (1963).

lines C with a line charge density $g(s)$. Separating the real and imaginary parts of $\chi(z)$,

$$\chi(x+iy)=\Phi(x,y)+i\Psi(x,y),\qquad(6)$$

the curves $\Phi(x,y)=$ const. are the equipotentials and thus Φ is an everywhere continuous function of z.[6] The curves $\Psi(x,y)=$ const. are the lines of force. The field strengths are

$$E_x=\partial\Phi/\partial x=\partial\Psi/\partial y\qquad(7)$$

$$E_y=\partial\Phi/\partial y=-\partial\Psi/\partial x\qquad(8)$$

by the Cauchy-Riemann relations. The charge distribution can be determined by evaluation of the line integral of the electric force around a closed curve. This gives

$$2\pi g(s)=\partial\Psi_r(s)/\partial s-\partial\Psi_l(s)/\partial s,\qquad(9)$$

where s is a natural coordinate along the curve $(ds^2=dx^2+dy^2)$ and the subscripts denote the right- and the left-hand side of the oriented line element. Finally, we note that

$$g(z^*)=g(z),\qquad(10)$$

and

$$\Phi(z^*)=\Phi(z),\qquad(11)$$

$$\Psi(z^*)=-\Psi(z),\qquad(12)$$

since the nonreal zeros z_i must occur in conjugate pairs.

For the van der Waals gas (1) the relation between the potential and the density is

$$\chi(z)=\rho/(1-\rho)-\nu\rho^2,\qquad(13)$$

by use of Eq. (3), and with

$$\nu\equiv a/kT.\qquad(14)$$

For convenience we use such units that $d=1$. Inserting the result (13) in Eq. (4) we find

$$\rho(dz/d\rho)=z[(1-\rho)^{-2}-2\nu\rho]\qquad(15)$$

with solution

$$z=\frac{\rho}{1-\rho}\exp\left[\frac{\rho}{1-\rho}-2\nu\rho\right].\qquad(16)$$

The infinite dilution limit, $\chi/z\rightarrow1$ when $z\rightarrow0$, determines the integration constant. The inverse function $\rho(z)$ as defined by (16) is multivalued, and by Eq. (13) the potential $\chi(z)$ will also be multivalued. These two equations form the basis for the subsequent discussion.

3. THE HEAD OF THE DISTRIBUTION

The branch points of the multivalued function $\rho(z)$ are given by $dz/d\rho=0$, or

$$2\nu\rho(1-\rho)^2=1.\qquad(17)$$

---

[6] This reflects that for each finite pole z_i the discontinuity across the cut associated with the corresponding logarithmic singularity in $\chi(z)$ is purely imaginary.
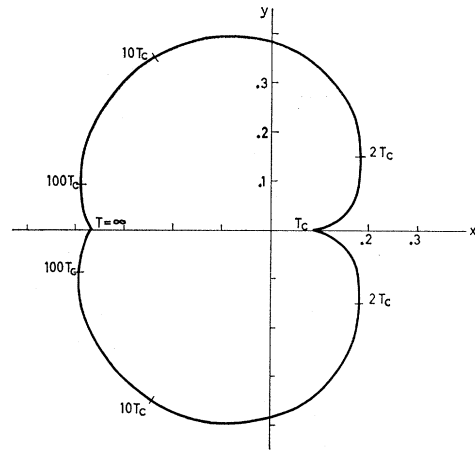

FIG. 2. The position of the head of the distribution for $T\geq T_c$.

The discontinuities in Ψ arise by choice of different sheets of the function ρ on the two sides of the charged line. An endpoint, or "head", of the line charge is thus a branch point of the function $\chi(z)$ (but not necessarily vice versa).

Let us now fix the attention on temperatures above the critical temperature. This corresponds to $\nu<\nu_c=27/8$. Equation (17), determining the branch points, is easily solved if we for convenience introduce a new parameter u instead of ν by

$$2\nu=\sin^33u/\sin^22u\sin u.\qquad(18)$$

The temperature interval (T_c,∞) then corresponds to the interval $(0,\pi/3)$ for u. By insertion one sees that (17) is satisfied by the two complex conjugate values

$$\rho_h=1-(\sin2u/\sin3u)e^{\pm iu},\qquad(19)$$

and one real and positive value

$$\rho=1+\sin u/\sin3u.\qquad(20)$$

The real value (20) corresponds to z real and negative. Near the origin one must have $\rho\sim z$, and it is not difficult to see that the set of ρ, z values given by (20) belongs to a branch of the function $\rho(z)$ that does not behave properly.

The remaining values (19) yield by Eq. (16) the following values for z:

$$z_h=\frac{1}{2e\cos u}\exp\left\{-\frac{\sin3u\cos4u}{2\cos u\sin2u}\right.$$

$$\left.\mp i\left(\frac{\sin3u\cos2u}{\cos u}-3u\right)\right\}.\qquad(21)$$

Figure 2 shows the location of these points as function of the temperature. At the critical temperature $(u=0)$ the two points close in onto the positive real axis at $z_c=\frac{1}{2}e^{-7/4}$, as expected. For $T\rightarrow\infty$ $(u\rightarrow\frac{1}{3}\pi)$, $z_h\rightarrow-1/e$. This is as it should be, because in this limit Eq. (13)
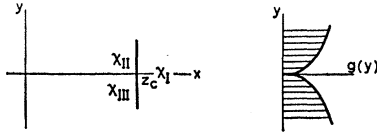
FIG. 3. The three branches of χ and the density of zeros near the real axis for the critical temperature.

reduces to $\chi^{\text{h.c.}}(z)$ for a gas of hard rods of unit length, whose zero distribution covers the interval $(-\infty, -1/e)$ on the real axis.[3] In the neighborhood of these limiting points we have approximately

$$z_h/z_c \simeq 1 + \frac{9\Delta T}{4T_c} \cdot \exp\left\{ \pm \frac{4i}{3}\left(\frac{\Delta T}{3T_c}\right)^{1/2} \right\},$$

$$\Delta T = T - T_c \ll T_c \quad (22)$$

and

$$ez_h \simeq -1 + \frac{3}{2}(2\nu)^{2/3} \exp(\pm \frac{2}{3}\pi i) \quad T \gg T_c. \quad (23)$$

4. CRITICAL TEMPERATURE

Let us study the zero distribution at the critical temperature T_c in the neighborhood of the point $z = z_c = \frac{1}{2}e^{-7/4}$ on the positive real axis. Putting $\nu = \nu_c = 27/8$ and

$$z = z_c + \hat{z} \quad (24)$$

in the basic Eqs. (13) and (16), we find

$$\hat{z}/z_c = 3^5 2^{-4}\hat{\rho}^3 - 3^6 2^{-6}\hat{\rho}^4 + O(\hat{\rho}^5) \quad (25)$$

$$\hat{\chi} = (\tfrac{3}{2})^4\hat{\rho}^3 - (\tfrac{3}{2})^5\hat{\rho}^4 + O(\hat{\rho}^5), \quad (26)$$

where

$$\hat{\rho} = \rho - \rho_c = \rho - \tfrac{1}{3}, \quad (27)$$

$$\hat{\chi} = \chi - \chi_c = \chi - \tfrac{1}{8}. \quad (28)$$

Elimination of $\hat{\rho}$ between Eqs. (25) and (26) yields

$$\hat{\chi} = \frac{\hat{z}}{3z_c} + (\tfrac{3}{2})^6\hat{\rho}^4 = \frac{\hat{z}}{3z_c} + (9/4)\left(\frac{2\hat{z}}{9z_c}\right)^{4/3}, \quad (29)$$

to this order. The first term on the right-hand side is a single-valued function of z, but the second term shows that $z = z_c$ is a branch point of order two. Putting

$$2\hat{z}/9z_c = \alpha e^{i\beta}, \quad (30)$$

where α is real and positive and $-\pi \leq \beta \leq \pi$, then the three branches of the function $\hat{\chi}$ are

$$\hat{\chi}_{\text{I}} = (3/2)\alpha e^{i\beta} + (9/4)\alpha^{4/3}e^{i4\beta/3}, \quad (31)$$

$$\hat{\chi}_{\text{II}} = (3/2)\alpha e^{i\beta} + (9/4)\alpha^{4/3}e^{i(4\beta+2\pi)/3}, \quad (32)$$

$$\hat{\chi}_{\text{III}} = (3/2)\alpha e^{i\beta} + (9/4)\alpha^{4/3}e^{i(4\beta-2\pi)/3}. \quad (33)$$

On the positive real z axis χ has to be real. Therefore the relevant branch to the right of $z = z_c$ (i.e., for $\beta = 0$) is χ_{I}. To the left we must have branch II above the real axis ($\beta = +\pi$) and branch III below ($\beta = -\pi$).

Now we have to ensure that $\Phi = \text{Re}\chi$ is continuous

everywhere. For $\beta > 0$, Eqs. (31) and (32) show that $\Phi_{\text{I}} = \Phi_{\text{II}}$ only for $\beta = \frac{1}{2}\pi$. Similarly below the real axis $\Phi_{\text{I}} = \Phi_{\text{III}}$ for $\beta = -\frac{1}{2}\pi$ only. This means that the charged line crosses the real axis at a right angle.

The discontinuity of $\Psi(y)$ across the line charge is easily found to be

$$\Delta\Psi = \Psi_{\text{I}} - \Psi_{\text{II}} = \tfrac{9}{2}\alpha^{4/3}\sin\frac{2\pi}{3} = (4e^7y^4/\sqrt{3})^{1/3} \quad (34)$$

for $y > 0$. By Eq. (9) the density of zeros close to the real axis is given by

$$g(y) = \frac{1}{2\pi}\frac{\partial\Delta\Psi}{\partial y} = \pi^{-1}2^{5/3}3^{-7/6}e^{7/3}y^{1/3} = 2.88\cdots y^{1/3}, \quad (35)$$

as shown in Fig. 3.

For completeness one easily assures oneself that *both* Φ and Ψ are continuous between branch II and branch III, so the real axis is not charged.

5. THE CHARGE DISTRIBUTION NEAR THE HEAD

In the immediate neighborhood of the head (21) of the distribution we can treat

$$z - z_h \equiv \hat{z} \equiv \alpha e^{i\beta} \quad (36)$$

as a small quantity, and for the potential $\hat{\chi} = \chi - \chi_h$ we find in the same way as in the previous section

$$\hat{\chi} = \frac{\hat{z}}{2\nu z_h(1-\rho_h)^2} - \frac{\sqrt{2}\hat{z}^{3/2}}{3\nu z_h^{3/2}(1-\rho_h)^{1/2}(3\rho_h - 1)^{1/2}} + \cdots, \quad (37)$$

where ρ_h and z_h are given by the Eqs. (19) and (21), respectively. The expansion is valid for $T_c < T < \infty$. In this case $\hat{z} = 0$ is a simple branch point. Written in terms of the variable u the second term on the right-hand side takes the form

$$\hat{\chi} - \frac{\hat{z}}{2\nu z_h(1-\rho_h)^2}$$

$$= \frac{8(\alpha e)^{3/2}\sin 2u \cos^2 u}{3\sin^2 3u(1+9\cot u)^{1/4}}\exp\left(\frac{3\sin 3u \cos 4u}{4\cos u \sin 2u}\right)$$

$$\times\exp\left\{\pm i\left[\tfrac{1}{2}\tan^{-1}(3\cot u)\right.\right.$$

$$\left.\left. + \frac{3\sin 3u \cos 2u}{2\cos u} - 4u - \frac{\pi}{2}\right] + \tfrac{3}{2}\beta i + k\pi i\right\}, \quad (38)$$

with k integer. The upper sign always refers to the upper half plane. The two branches differ with π in the argument. It follows that the real part Φ of the function takes the same value for both branches if and only if the argument for each branch equals $n\pi/2$, where n is odd. This determines $\beta = \beta_h(u)$, and thus the direction

of the line charge near the head. We find

$$\beta_h = \mp\left[\frac{1}{3}\tan^{-1}(3\cot u) - \frac{8}{3}u + \frac{\sin 3u\cos 2u}{\cos u} - \frac{2\pi}{3}\right]. \quad (39)$$

In order to fix the above integer n we have used the previous result $\beta_h = \pm\frac{1}{2}\pi$ at the critical temperature $(u=0)$. The variation of this direction with the temperature is sketched in Fig. 4.

The imaginary part of χ, Eq. (38), determines how the density distribution behaves in terms of α, the distance from the head. By Eq. (9)

$$g(\alpha) = \frac{1}{2\pi}\frac{\partial\Delta\Psi}{\partial\alpha} = \frac{4\sin 2u\cos^2 u}{\pi\sin^2 3u(1+9\cot^2 u)^{1/4}}$$

$$\times\exp\left[\frac{3}{2} + \frac{3\sin 3u\cos 4u}{4\cos u\sin 2u}\right]\alpha^{1/2}. \quad (40)$$

The coefficient in front of $\alpha^{1/2}$ increases without bound both for $T\to T_c$ and for $T\to\infty$, indicating the lack of validity of the expansion (37) for these limiting values.

Note especially that for very high temperatures the direction of the distribution tends to

$$\beta_h(T\to\infty)\to\pm(13/9)\pi. \quad (41)$$

For high temperatures it thus seems that the charged line starting from the head in the upper half-plane would meet the corresponding line in the lower half-plane in a point Y on the real axis near $z = -1/e$. In the next section this high-temperature behavior is examined in more detail.

6. HIGH TEMPERATURES

In the case $T\gg T_c$, i.e., $\nu\ll 1$, we study the neighborhood of $z=-1/e$ by setting
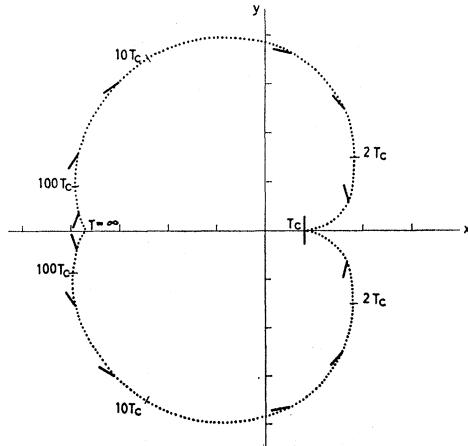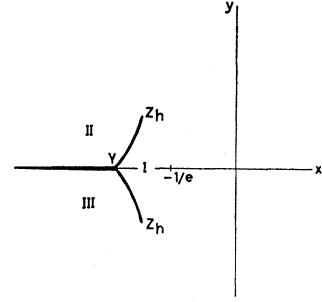
$$ez = -1 + \zeta\nu^{2/3}. \quad (42)$$

FIG. 4. The direction of the line of zeros near the head.

FIG. 5. The three branches of χ for high temperatures.

Using Eq. (16), one easily finds that this region to lowest order in ν corresponds to

$$1 - \rho = \mu^{-1}\nu^{-1/3}, \quad (43)$$

with

$$\zeta = \frac{1}{2}\mu^2 - 2\mu^{-1}. \quad (44)$$

If we denote real and imaginary parts by subscripts then (44) is equivalent to

$$\zeta_r = -2\mu_r(\mu_r^2 + \mu_i^2)^{-1} + \frac{1}{2}\mu_r^2 - \frac{1}{2}\mu_i^2, \quad (45)$$

and

$$\zeta_i = \mu_i[2(\mu_r^2 + \mu_i^2)^{-1} + \mu_r]. \quad (46)$$

The corresponding expansion of the potential (13) reads

$$\chi = -1 + (\mu - \mu^{-2})\nu^{1/3} + \cdots, \quad (47)$$

or

$$\Phi = -1 + [\mu_r + (\mu_i^2 - \mu_r^2)(\mu_r^2 + \mu_i^2)^{-2}]\nu^{1/3}, \quad (48)$$

$$\Psi = \mu_i[1 + 2\mu_r(\mu_r^2 + \mu_i^2)^{-2}]\nu^{1/3}. \quad (49)$$

The position of the head z_h of the charged line is the singular points of $\mu(\zeta)$, Eq. (44). We find for the relevant zeros of $d\zeta/d\mu = \mu + 2\mu^{-2}$:

$$\mu_h = 2^{1/3}e^{\mp\pi i/3}, \quad\text{i.e.,}\quad \zeta_h = 3\times 2^{-1/3}e^{\pm 2\pi i/3}, \quad (50)$$

in agreement with Eq. (23).

In order to determine the intersection point Y of Fig. 5, let us focus the attention on the real axis. By Eq. (46) z is real for three different values of μ_i:

I.

$$\mu_i = 0, \quad (51)$$

$$\zeta_r = \frac{1}{2}\mu_r^2 - 2\mu_r^{-1}, \quad (52)$$

$$\Phi = -1 + (\mu_r - \mu_r^{-2})\nu^{1/3}, \quad (53)$$

$$\Psi = 0. \quad (54)$$

II and III.

$$\mu_i = \pm(-2\mu_r^{-1} - \mu_r^2)^{1/2}, \quad (55)$$

$$\zeta_r = \mu_r^{-1} + 2\mu_r^2, \quad (56)$$

$$\Phi = -1 + \frac{1}{2}(\mu_r - \mu_r^4)\nu^{1/3}, \quad (57)$$

$$\Psi = \pm\frac{1}{2}[-(2+\mu_r^3)^3\mu_r^{-1}]^{1/2}. \quad (58)$$

The two last solutions exist only if $-2^{1/3}\le\mu_r < 0$, so that for $\zeta > -3\times 2^{-1/3}$ solution I must be chosen. This is in accordance with the exact solution[3] for $\nu=0$, which
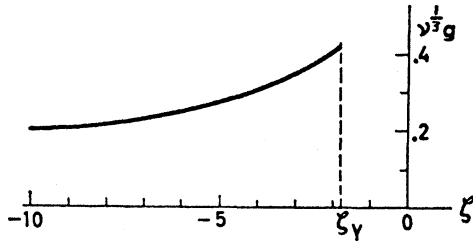
FIG. 6. Density of zeros on the real axis for high temperatures.

shows that $\Psi=0$ for $x>-1/e$, $y=0$, $\Psi>0$ for $x<-1/e$, $y=0+$, and $\Psi<0$ for $x<-1/e$, $y=0-$.

The location of the point Y is determined by

$$\Phi_I(z_Y)=\Phi_{II}(z_Y)=\Phi_{III}(z_Y), \quad (59)$$

or by Eqs. (53) and (57),

$$2\mu_r(I)-2\mu_r^{-2}(I)=\mu_r(II)-\mu_r^4(II). \quad (60)$$

Comparing Eqs. (52) and (56) we see that

$$\mu_r(I)=-2\mu_r(II) \quad (61)$$

corresponds to the same point in the z plane, and it is not difficult to show that the other solutions of the equation $\zeta(I)=\zeta(II)$ must be discarded. Solving the last two equations we obtain

$$\mu_r(II)=-(5+3\sqrt3)^{-1/3}, \quad (62)$$

and hence

$$\zeta_Y=-(3+3\sqrt3)(5+3\sqrt3)^{-2/3}=-1.7430\cdots. \quad (63)$$

The point Y therefore moves to the left with decreasing temperature as

$$z_Y=-0.3679-0.6412\nu^{2/3}. \quad (64)$$

The charge densities on the three lines coming together in Y are also functions of the temperature. Since $\Psi \propto \nu^{1/3}$ and $d\zeta/dz=e\nu^{-2/3}$, it follows by Eq. (9) that $g \propto \nu^{-1/3}$, decreasing with decreasing temperature. On the real axis to the left of the point Y, Eqs. (9) and (58) yield

$$g=(e/2\pi)\nu^{-1/3}[-\mu_r(2+\mu_r^3)]^{1/2}, \quad (65)$$

where $-(5+3\sqrt3)^{-1/3}\leq\mu_r(z)<0$ is given by Eq. (56).

7. LOW TEMPERATURES

Now we consider temperatures so far below T_c that $\nu=a/kT$ can be treated as a large parameter. It follows from the equation of state that for very low temperatures the fugacity z that corresponds to the saturated vapor line is very small, and that the corresponding densities ρ_g and ρ_l of the gas and the liquid are close to 0 and 1. This means that in the complex z plane the line charge crosses the positive real axis to a point very close to the origin. Moreover, the two branches of the function $\chi(z)$ on each side of the line charge are obtained for ρ close to 0 and 1, respectively.

Let us therefore study the function $z(\rho)$, Eq. (16), in these two limiting cases. For $2\nu\rho\ll1$ we have

$$z=\rho+O(\rho^2), \quad (66)$$

or inverted

$$\rho=z+O(z^2). \quad (67)$$

In the other case, $1-\rho\ll1$, we get to lowest order

$$z=(1-\rho)^{-1}\exp[(1-\rho)^{-1}-2\nu] \quad (68)$$

or, approximately,

$$(1-\rho)^{-1}=2\nu+\ln z. \quad (69)$$

The corresponding approximations for the potential (13) read

$$\chi_g\simeq\rho\simeq z, \quad (2\nu\rho\ll1) \quad (70)$$

and

$$\chi_l\simeq(1-\rho)^{-1}-\nu\simeq\nu+\ln z \quad (1-\rho\ll1). \quad (71)$$

Putting $z=re^{i\phi}$, and requiring continuity of the real part of χ, we obtain for the position of the line charge

$$r\cos\phi=\nu+\ln r \quad (72)$$

or

$$r=e^{-\nu}e^{r\cos\phi}\simeq e^{-\nu}(1+e^{-\nu}\cos\phi), \quad (73)$$

to this order of accuracy. The corresponding ρ values are of the order of $e^{-\nu}$ and $1-\nu^{-1}$, showing the validity of the expansions.

In this approximation, therefore, the charge is distributed on a closed curve deviating only slightly from a circle with radius $e^{-\nu}$ around the origin. The lines of force are by Eqs. (70) and (71) given by

$$\Psi_g=r\sin\phi; \quad \Psi_l=\phi \quad (74)$$

and sketched in Fig. 8. Using the fact that Ψ_g is negligible, we obtain for the charge density
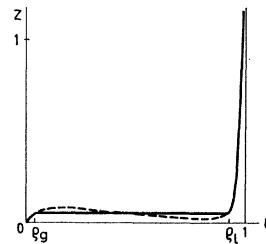
$$g(z)=e^\nu/2\pi. \quad (75)$$

In this zeroth approximation the total charge is uniformly distributed on the closed curve.

In the same way one can of course carry the calculation to higher order. As long as exponentially small terms in the density are neglected, only χ_l is needed, and as a better approximation we find[7]

$$\chi_l=\nu+\ln z-\ln(2\nu+\ln z). \quad (76)$$

On the charged curve the imaginary part of this becomes

$$\Psi_l=\phi(1-\nu^{-1}), \quad (77)$$

FIG. 7. The fugacity z as function of the density ρ for low temperatures.

---

[7] As a check, Eq. (76) yields the approximate values $\rho_l\simeq1-\nu^{-1}$, $\rho_g\simeq\nu e^{-\nu}$, which agrees with the liquid and gas densities one finds at very low temperatures by Maxwell's rule.

from which the density

$$g_c = e^\nu (1 - \nu^{-1})/2\pi \qquad (78)$$

follows. The total charge on the curve thus equals $2\pi e^{-\nu} g_c = 1 - \nu^{-1}$. The small rest of the charge lies on the negative real axis. Here the imaginary part of χ, Eq. (76), has the form

$$\Psi(y = 0\pm) \simeq \pm \left[\pi - \tan^{-1} \frac{\pi}{2\nu + \ln(-x)} \right]$$

$$\simeq \pm \pi \left[1 - \frac{1}{2\nu + \ln(-x)} \right]. \qquad (79)$$

The corresponding density is by Eq. (9)

$$g_{\text{axis}}(x) = \frac{1}{2\pi} \frac{\partial}{\partial x} [\Psi(y = 0^-) - \Psi(y = 0^+)]$$

$$= \frac{1}{(-x)[2\nu + \ln(-x)]^2}. \qquad (80)$$

It is easily checked that the total charge on the real axis just equals the remaining part ν^{-1} of the total charge:

$$\int_{-\infty}^{-e^{-\nu}} dx \, g_{\text{axis}}(x) = \nu^{-1} = \frac{kT}{a}. \qquad (81)$$

For $T \to 0$ this part disappears linearly, and the total charge approaches a uniform distribution on a circle whose diameter decreases exponentially towards zero.

8. CONCLUDING REMARKS

We have determined the main features of the zero distribution corresponding to the van der Waals equation of state. The zero line was fixed by the continuity requirement of the real part of the multivalued function $\chi(z)$, whereupon the discontinuity of the imaginary part of $\chi(z)$ determined the actual value of the density of zeros. By the same procedure one could clearly obtain all quantitative details by numerical calculation, if desired. It should be noted that the Maxwell rule is not a separate requirement, but included in this general procedure.

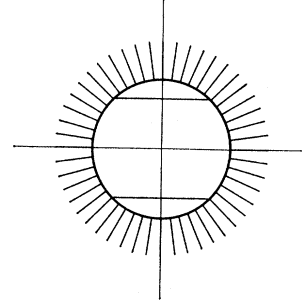The resulting distribution of zeros is much more complex than in the case of lattice gases with attractive

Fig. 8. Lines of force at low temperatures.

interaction ($\phi_{ii} = +\infty$, $\phi_{ij} < 0$ for $i \neq j$). For these Lee and Yang[2] proved that all zeros z_n have the same modulus

$$|z_n| = \exp(\tfrac{1}{2} \sum_j{}' \phi_{ij}/kT), \qquad (82)$$

approaching zero when $T \to 0$ in the same way as in our case. A lattice gas analogue of van der Waals' equation is obtained for a very weak attraction of very long range, yielding the equation of state[8,9]

$$p/kT = -\ln(1 - \rho) - \nu \rho^2, \qquad (83)$$

with

$$kT = a = -\tfrac{1}{2} \sum_i{}' \phi_{ij}. \qquad (84)$$

Analytic results for the angular distribution $G(\phi) = 2\pi e^{-\nu} g$ on the circle $|z| = e^{-\nu}$ were obtained by Katsura.[4]

Van der Waals' equation (1) and Eq. (83) are both equations of state for models with an attractive tail $\gamma \phi(\gamma r)$ considered in the limit when the range $1/\gamma \to \infty$. An analysis of the distribution of zeros for very small, but finite values of γ would be of interest. The point is that while one can prove the nonexistence of a phase transition in one dimension for any finite γ,[9] an expansion in powers of γ yields a phase transition to every order, with (1) or (83) as the zeroth order equation of state.[5] This means that the expansion for small γ and $T < T_c$ cannot be a pointwise approximation method for the density of zeros: On the positive real axis $g = 0$, but it is approximated by distributions that cross the real axis with finite density. The nature of this gap in the line of zeros presents an unsolved problem.

[8] T. L. Hill, *Statistical Mechanics* (McGraw-Hill Book Company, Inc., New York, 1956), Sec. 46.
[9] M. Kac, Phys. Fluids 2, 8 (1959) and further unpublished calculations.